water

MDPI

Article

Propagation of Uncertainty in Multi-Source Elevation Models into Hydrological Modelling and Sediment Connectivity in a Loess Catchment

Waldemar Kociuba * and Iga Zdanowicz

Institute of Earth and Environmental Sciences, Faculty of Earth Sciences and Spatial Management, Maria Curie-Sklodowska University in Lublin, Al. Krasnicka 2 D, 20-718 Lublin, Poland
* Correspondence: waldemar.kociuba@umcs.pl; Tel.: +48-81-5376853

Abstract

The accuracy and resolution of digital elevation models (DEMs) determine the reliability of outputs used in hydrological modeling. However, an assessment of their suitability should not be limited to vertical accuracy alone. Particularly in small, highly fragmented catchments, uncertainty in elevation representation can propagate to subsequent derivatives depending on the local topographic structure and, consequently, influence the interpretation of runoff organization and sediment transport. The aim of this study is to determine how differences between multi-source elevation models propagate from the underlying elevation representation through slope and runoff organization to the drainage network and the spatial pattern of sediment connectivity. In the Stocki Creek catchment in the Lublin Uplands (SE Poland), ASTER GDEM, SRTM, EU-DEM, and a local TIN model were compared. Aerial laser scanning (ALS) data were used as a high-resolution reference for validating elevation and derived outputs. Vertical accuracy was assessed using RMSE and NMAD, and then the representation of relief, slope, hydrologic routing outputs, the drainage network, and the Sediment Connectivity Index (SCI) were compared. The smallest discrepancies relative to ALS were obtained for the TIN (RMSE 1.48 m; NMAD 0.41 m), and the largest for ASTER (6.78 m; 2.37 m). Errors were highest in forested areas. All models reproduced the general elevation pattern of the watershed relatively well, whereas differences were much more pronounced in products dependent on local gradients and topographic continuity. Satellite models smoothed out the steep slopes of gullies, generalized short runoff lines, and led to a simplification of the spatial pattern of sediment connectivity. The results show that the usefulness of elevation models in hydrological applications should be assessed not only by their vertical accuracy but also by the propagation of uncertainty to subsequent processed products. Validation against ALS therefore allows for an assessment of the reliability of multi-source Earth Observation (EO) products throughout the entire analytical chain: from elevation, through local morphometry and runoff routing, to the drainage network and sediment connectivity.

Keywords: remote sensing; digital elevation model—DEM; ALS; DEM uncertainty; uncertainty propagation; hydrological modelling; flow routing; drainage network; sediment connectivity; loess catchment

Check for updates

Academic Editors: Min-Cheng Tu, Hong-Yuan Huo and James Deemy

Received: 11 September 2026
Revised: 5 October 2026
Accepted: 17 October 2026
Published: 22 October 2026

Copyright: © 2026 by the authors. Licensee MDPI, Basel, Switzerland. This article is an open access article distributed under the terms and conditions of the Creative Commons Attribution (CC BY) license.

1. Introduction

Digital Elevation Models (DEMs) and Digital Terrain Models (DTMs) are the primary source of topographic information for hydrological modeling and hydrogeomorphological

analyses. They are used to determine, among other things, slope, runoff directions and accumulation, watershed boundaries, drainage networks, and the topographic components of erosion and sediment transport indices. The impact of DEM quality on the results of hydrological analyses has been known for many years [1,2], and recent studies show that resolution, vertical accuracy, land cover, and the method of surface representation are all important factors [3–9]. Particularly in forests, errors in global models may be associated with the incomplete removal of vegetation effects, which has spurred the development of bare-earth models, such as Forest And Buildings removed Copernicus DEM (FABDEM) [10], and new methods for correcting and validating global DEMs [11,12].

Uncertainty, however, is a broader issue than elevation accuracy alone and is an inherent characteristic of products derived from Earth Observation (EO) data. Its significance depends both on the properties of the source data and on the subsequent processing steps, as well as on the type of derived product. For example, Hong et al. [13], in their analysis of land cover classification from multi-temporal Sentinel-2 imagery, demonstrated that the uncertainty of the results depends on the parameters and organization of the remote sensing data processing workflow. Although this issue pertains to a different type of EO product, it highlights a broader need to assess not only the quality of the input data but also the stability of the information obtained in subsequent stages of processing.

In hydrological applications, this topic is particularly important because remote sensing products are increasingly being directly integrated into the modeling of catchment processes. Yu et al. [14] demonstrated that an appropriate spatial representation of information derived from remote sensing data can be crucial for runoff simulation and the spatial representation of hydrological processes. In the case of elevation models, the problem takes on an additional dimension: errors or generalizations present in the original elevation field are not limited to elevation itself but can be carried over to products derived from it, such as slope, runoff direction and accumulation, drainage networks, and sediment connectivity indices.

The ASTER GDEM and SRTM models are among the most widely used global elevation products derived from remote sensing [15,16]. Their nominal resolution of approximately 30 m allows for regional analyses but may lead to the generalization of narrow valleys, gorges, gullies, and short drainage lines. The EU-DEM integrates satellite sources and serves as an intermediate step between classic global DEMs and newer Copernicus products. Recent validations indicate that new global products are becoming increasingly accurate, but vertical accuracy alone is insufficient to assess their hydrological suitability; the quality of the representation of the runoff network and local gradients is also crucial [7,8]. From a hydrological modeling perspective, an accurate representation of topography remains a prerequisite for reliable routing and catchment delineation [17].

Research to date has provided extensive knowledge regarding the vertical accuracy of global DEMs and the impact of their resolution on selected hydrological analyses. However, less attention has been focused on a systematic assessment of how differences between multi-source elevation models are revealed at successive levels of the analytical chain, as one moves from basic elevation data to models that are increasingly dependent on local gradients, surface continuity, and the organization of flow paths. From the perspective of practical hydrological applications, it is therefore important not only to ask which DEM has the smallest vertical error, but also whether relatively small or spatially localized differences in elevation lead to significant changes in the process-derived models based on topography.

In this study, we analyze four models under evaluation: ASTER GDEM, SRTM, EU-DEM, and TIN. ALS data from the Information System for Country Protection (ISOK) [18] project were adopted as an independent, high-resolution reference dataset. This separation of the evaluated data from the reference dataset makes it possible to trace the propagation of

differences within a common framework: elevation → slope → runoff routing → drainage network → sediment connectivity. This framework does not assume that each subsequent product must exhibit a linearly or monotonically increasing error. Rather, it serves to verify whether products that are increasingly dependent on local geometry and topographic continuity exhibit greater sensitivity to the quality and resolution of the elevation model than the elevation representation at the catchment scale itself.

The main research question is therefore: how are the differences among multi-source elevation models reflected in increasingly process-dependent outputs used in hydrological modeling and the assessment of sediment connectivity in a small loess catchment? We examine the extent to which elevation models derived from different data sources and acquisition and processing methods reproduce the general elevation structure of the catchment, and how differences among these models become expressed in products dependent on local gradients and topographic continuity, particularly in slope, runoff patterns, the drainage network, and the spatial pattern of sediment transport. These differences are interpreted as the combined effect of the data source, the method of data acquisition and processing, and the spatial resolution of the DEM, rather than as the consequence of any single factor. The study therefore adopts a cross-platform comparative validation framework and focuses not so much on ranking the vertical accuracy of individual DEMs as on assessing how differences among elevation datasets are reflected in subsequent levels of hydrological information.

To answer the research question, analyses were conducted in the Stocki Creek watershed on the Nałęczów Plateau (Lublin Upland; SE Poland). First, the vertical accuracy of ASTER, SRTM, EU-DEM, and TIN was evaluated relative to ALS, and then the geomorphometric and hydrological products generated using an identical processing scheme were compared. ALS serves as a consistent reference dataset in subsequent stages, allowing agreement in the general elevation representation to be compared with the agreement observed for products dependent on local topography and runoff patterns. Importantly, the observed differences among the derived products cannot be attributed exclusively to elevation error or spatial resolution, because the DEMs also differ in their source data and acquisition and processing methods. Moreover, because the DEMs were analyzed at their original spatial resolutions rather than normalized to a common grid resolution, the independent contribution of spatial resolution cannot be isolated from the effects of the other dataset characteristics. This approach addresses the growing need to integrate remote sensing observations with watershed modeling and to explicitly account for input data uncertainties in the interpretation of hydrological results [14].

2. Materials and Methods

2.1. Study Area

The study was conducted in the Stocki Creek catchment area in the western part of the Nałęczów Plateau (Lublin Upland) (Figure 1A). The catchment area covers approximately 17 km^2, and Stocki Creek flows into the Bystra River (right tributary of the Vistula River). The landform is typical of the loess areas of the Lublin Upland, where the susceptibility of loess to erosion, the development of a gully network, and the strong interplay between slope processes and runoff are well documented (Figure 1A). Regional studies have shown both high spatial variability in gully density [19] and the significance of spring thaw events and torrential rainfall for erosion [20]. Reconstructions of the development of gully systems point to a long-term interaction between natural and anthropogenic factors [21–24].

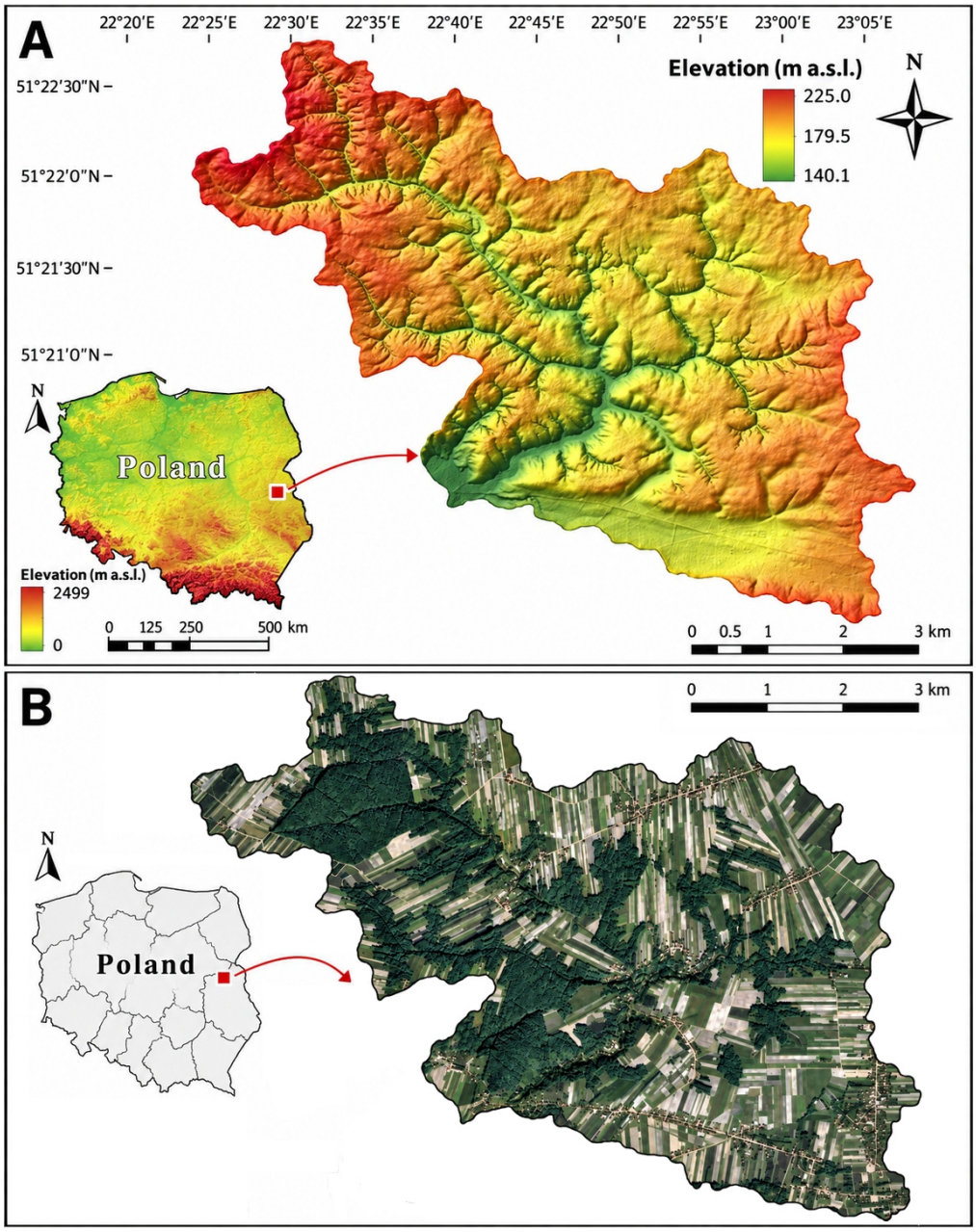

Figure 1. Location of the study area. (**A**) Location of the Stocki Creek catchment. (**B**) Orthophoto map of the study area. Source: GUGIK: https://mapy.geoportal.gov.pl/imap/Imgp_2.html; accessed on 9 September 2026; spatial resolution: 10 m.

The Nałęczów Plateau is a mesoregion of the Lublin Uplands and a classic area of loess landforms. Locally, the density of the gully network reaches 10 km/km^2, and relative heights exceed 100 m [19,25]. This morphology is the result of both natural erosion processes and centuries of land use (Figure 1B). Regional literature documents the development of road and field gullies associated with land-use patterns [26,27], historical phases of erosion and sedimentation [23,28], and contemporary changes in loess landforms. Such intense fragmentation poses a challenging test for elevation models of varying resolutions.

The morphological axis of this part of the region is the Bystra Valley. In the analyzed part of the catchment, gentle slopes predominate on the uplands, while steep slopes are concentrated within the valleys and gullies.

Agricultural land covers approximately 11.74 km^2 (about 70% of the catchment area), while forests cover approximately 4.21 km^2 (about 25%) and are concentrated mainly in

areas prone to gully erosion (Figure 1B). The importance of land use for the development of loess landforms is well recognized in the Lublin Uplands [22,27]. More recent studies also emphasize the role of land-use changes in the development of sinkholes and piping-type features [29] as well as the need to integrate geomorphological, environmental, and functional values into the management of gullies at the interface between rural and urban areas [30]. Variations in land cover were taken into account in the interpretation of elevation errors.

2.2. Evaluated Models

Four elevation models representing different data sources and acquisition methods were used for comparison: ASTER GDEM V003, SRTM V003, EU-DEM v1.1, and a local TIN model. Since the data sources and structures differ among the models, the comparison focuses on their practical usefulness as ready-to-use elevation representations, rather than solely on the impact of the TIN/raster format. A comparison of the spatial representations of the four evaluated models and the ALS reference is shown in Figure 2A–F.

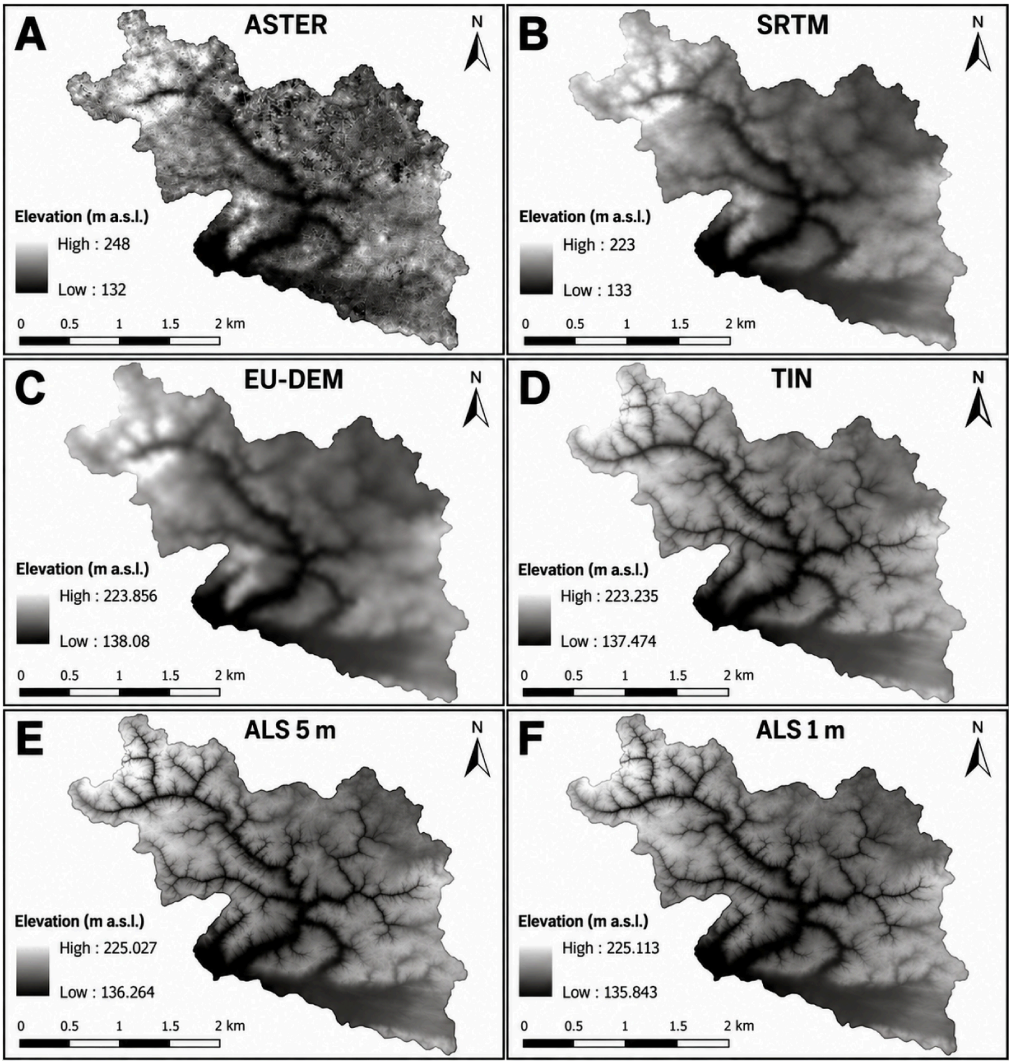

Figure 2. Comparison of elevation models of the study area: (**A**) ASTER GDEM V003, (**B**) SRTM V003, (**C**) EU-DEM v1.1, (**D**) TIN, (**E**) 5-m reference ALS DTM, and (**F**) 1-m reference ALS DTM.

2.2.1. ASTER GDEM V003

ASTER GDEM V003 (Version 3; Sensor Information Laboratory Corporation (SILC), Tokyo, Japan) is a global elevation model derived from stereoscopic images captured by the

ASTER sensor. For the study area, the raster resolution is 27.78 m (Figure 2A). The model may contain artifacts associated with the imaging and processing; the characteristics of the GDEM version and its limitations are described by Abrams et al. [16]. The validity of ASTER was assessed directly against ALS reference data.

2.2.2. SRTM V003

SRTM NASA Jet Propulsion Laboratory (JPL), (Pasadena, CA, USA) is a global elevation model derived from radar interferometry. The mission, data acquisition method, and product characteristics are described by Rabus et al. [15]. In version V003, some data gaps were filled, and the product is available globally at a resolution 27.78 m (Figure 2B).

2.2.3. EU-DEM v1.1

EU-DEM v1.1 (Version 1.1; European Environment Agency (EEA), Copenhagen, Denmark) is a European hybrid product created by integrating SRTM and ASTER GDEM data. A 25-m-resolution raster was used for the analyzed area (Figure 2C). The product's characteristics and distribution are documented by the Copernicus Land Monitoring Service [31]. Including the EU-DEM along with its component models allows us to verify whether the integration of sources reduces the discrepancies observed in individual global DEMs. The spatial representation of the EU-DEM v1.1 elevation data is shown in Figure 2C.

2.2.4. TIN

The local TIN model was obtained from Head Office of Geodesy and Cartography (GUGiK, Warsaw, Poland) resources [18]. The irregular triangle mesh is based on elevation points and allows for a more detailed representation of terrain relief than global rasters. For raster analyses, the model was resampled to a 5-m grid (Figure 2D). For the source data used to construct this product, GUGiK materials reported an average elevation error of 0.8–2.0 m [32]. A comparison of the TIN with satellite models should be interpreted as a comparison of complete products from different sources, rather than a test of the interpolation method itself.

2.3. ALS-Derived Reference Data

The Airborne Laser Scanning (ALS) data were obtained from the national elevation data repository created as part of the ISOK project, one of whose key products was elevation data acquired using ALS technology [18]. The point cloud used in this study had a density of approximately 4 points/m^2 and was used to create a 5-m-resolution DTM (Figure 2E) and a 1-m-resolution reference DTM (Figure 2F). The 1-m-resolution raster was generated in ArcGIS Desktop 10.8 (Esri, Redlands, CA, USA) using the LAS Dataset to Raster tool, with cell-level averaging and missing value interpolation using the nearest-neighbor method. ISOK data were used as reference LiDAR data in geomorphometric studies of loess areas [33], and high-resolution laser scanning is an effective tool for the quantitative assessment of changes in gully landforms [34,35]. In this study, ALS is not treated as a fifth model to be evaluated, but rather as a high-resolution reference for validating ASTER, SRTM, EU-DEM, and TIN.

2.4. Data Processing and Standardisation

Before comparison, all data were cropped to a common analysis extent and converted to the PL-1992 national rectangular plane coordinate system (EPSG: 2180), based on the GRS80 ellipsoid. This was necessary because the source products use different reference systems (including WGS84 for ASTER GDEM and SRTM, and ETRS89 for EU-DEM). The nominal spatial resolution of each DEM under assessment was retained; the models were not resampled to a single common cell size, so as not to eliminate differences arising from

their actual resolution. Auxiliary layers requiring raster alignment, in particular the C-factor, were aligned to the grid of the DEM currently under analysis using the Resample tool in ArcGIS. The ModelBuilder diagram documents the target cell size for individual variants. Prior to the hydrological analyses, each DEM was subjected to a Fill operation. All subsequent calculations were performed in ArcGIS Desktop 10.8 (Esri, Redlands, CA, USA).

2.5. Assessment of Elevation Consistency with ALS

From the reference DTM created from ALS/ISOK data, 350 control points were selected and distributed across the catchment area (Figure 3). In the original scheme, 340 points were generated at random, and 10 were added to improve spatial coverage. For each point, the elevation difference $\Delta z_i = zDEM_{,i} - zALS_{,i}$ was calculated.

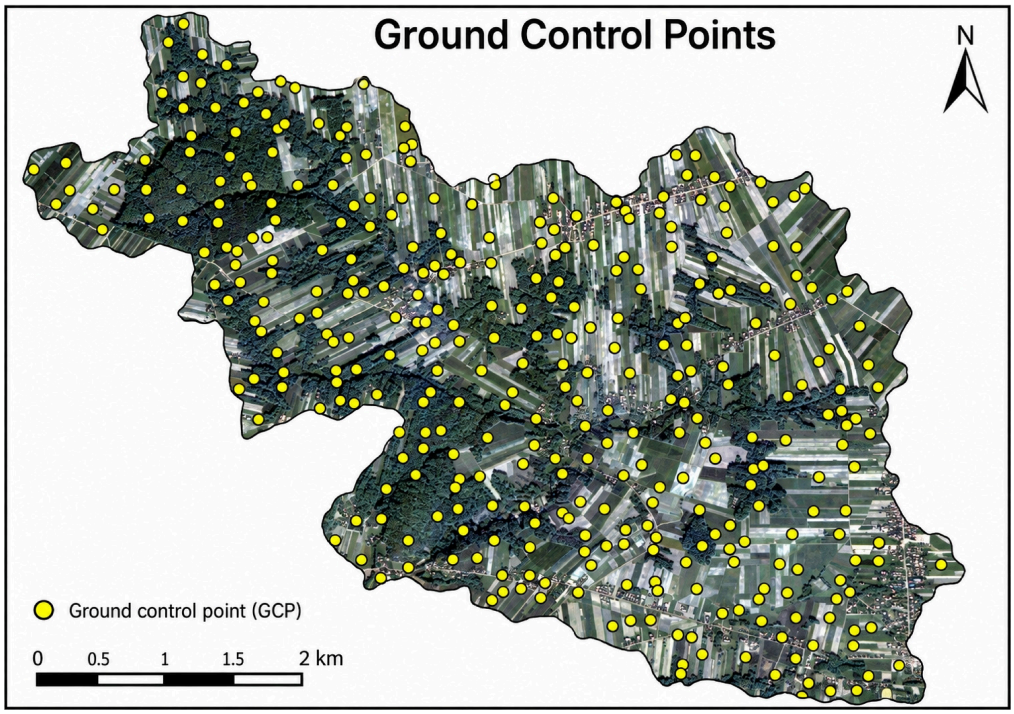

Figure 3. Distribution of the 350 control points used to assess the elevation consistency of the ASTER, SRTM, EU-DEM and TIN models against the reference ALS DTM.

Vertical accuracy was assessed using the RMSE and the robust NMAD measure, in accordance with DEM validation practice [3,36]. The RMSE was calculated as:

Equation (1):

$$\mathrm{RMSE} = \sqrt{\left[(1/n)\Sigma_{i=1}{}^{n}(\Delta z_i)^2\right]} \quad (1)$$

where n = 350 denotes the number of control points, $zDEM_{,i}$ is the elevation of the model under assessment at point i, $zALS_{,i}$ is the elevation of the ALS reference DTM, and Δz_i denotes the difference in elevation. The normalized median absolute deviation (NMAD) was used as a robust measure of error dispersion:

Equation (2):

$$\mathrm{NMAD} = 1.4826 \times \mathrm{mediana}(\,|\,\Delta z_i - \mathrm{mediana}(\Delta z)\,|\,) \quad (2)$$

where the factor 1.4826 scales the median absolute deviation so that, for a normal distribution, it is comparable to the standard deviation. RMSE and NMAD were reported in metres; NMAD is less sensitive to outliers and non-normal distributions of elevation errors [36].

2.6. Geomorphological and Hydrological Analyses

Prior to the hydrological analyses, all models were subjected to the same sequence of operations in accordance with the following workflow: Fill → Flow Direction → Flow Accumulation (Figure 4). Geomorphometric and hydrological products were then calculated whilst maintaining the nominal cell size of the given DEM. This approach allows for an assessment of the practical impact of the quality and resolution of the final elevation outputs on the modelling results (Figure 4).



Figure 4. Study framework and flowchart for calculating the Sediment Connectivity Index (SCI) implemented in ArcGIS ModelBuilder. The diagram shows the variant for SRTM; the same calculation procedure and parameterisation rules were applied to ASTER GDEM, EU-DEM, TIN and the reference ALS-DTM. The C-coefficient raster served as a common weighting layer, and the final SCI was calculated as the log10 of the ratio of the upslope and downslope components.

The geomorphometric analyses included hypsographic curves, slope gradient and aspect. The hypsographic curves were generated from the proportion of the surface area falling within successive elevation classes. Slope and aspect were calculated from each DEM in ArcGIS Desktop (Version 10.8; Esri, Redlands, CA, USA) using identical tool settings; slope was expressed in degrees and aspect in azimuths of 0–360° (flat cells: −1).

In the hydrological analyses, the direction and accumulation of runoff, catchment boundaries and the potential drainage network were determined. The catchment boundary was additionally compared with the Hydrographic Division Map of Poland (MPHP; State Water Holding Polish Waters, Warsaw, Poland), whilst the result obtained from ALS remained the primary reference for the derived outputs.

The catchment was delineated using the Watershed tool (Spatial Analyst → Hydrology, ArcGIS Desktop 10.8) based on the Flow Direction raster and a common outflow point. The same catchment-closing point was used for all models, meaning that any differences in the boundaries result from the topography of the DEM and the propagation of errors into the flow direction.

The drainage network was delineated from the Flow Accumulation raster, using a threshold of 1000 inflow cells, in line with the archived ModelBuilder model (Figure 4). The same numerical threshold was applied to all DEM variants. As the physical area represented by 1000 cells depends on the raster resolution, the comparison of network length and density was interpreted as an assessment of the practical performance of the products at their nominal resolution, rather than as a comparison of networks initiated from an identical catchment area.

SCI was calculated according to the approach of Borselli et al. [37], within the geomorphometric framework developed by Cavalli et al. [38]. The complete workflow used in ArcGIS ModelBuilder is shown in Figure 4. For each pixel, the following were calculated:

Equations (3)–(5):

$$IC = \log_{10}(D_up/D_dn) \quad (3)$$

$$D_up = \overline{W} \times \overline{S} \times \sqrt{A} \quad (4)$$

$$D_dn = \Sigma_i \left[d_i/(W_i \times S_i)\right] \quad (5)$$

where A is the catchment area upstream of the cell under analysis, $\overline{W}$ and $\overline{S}$ denote, respectively, the weighted mean weighting coefficient and the weighted mean slope of the upslope portion, d_i is the length of the runoff path segment in cell i, W_i is the local weighting coefficient, and S_i is the local slope. The land cover and land use coefficient C (C-factor; Figure 5) from the pan-European ESDAC/JRC layer, developed for RUSLE on the basis of data on land use, vegetation cover and agricultural practices [39]. The same C raster was applied to all DEMs, after adjusting the cell size to that of the model currently under analysis. Consequently, differences in SCI values result primarily from changes in the representation of topography, rather than from changes in the land cover layer.

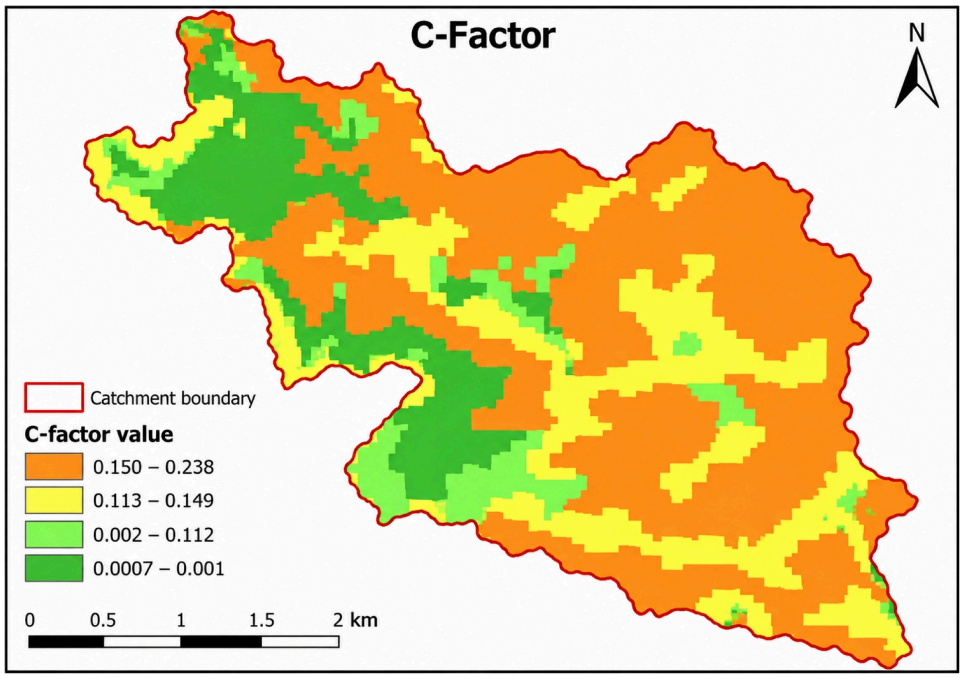

Figure 5. Spatial distribution of the C coefficient (cover-management factor) within the catchment, used as a common weighting layer in the SCI calculations; data source: ESDAC/JRC, methodology by Panagos et al. [39].

3. Results

3.1. Height Consistency of the Models with the ALS Reference

A comparison with the ALS DTM reference data revealed significant variations in the height consistency of the models (Table 1; Figure 6). The greatest discrepancies were found for ASTER (RMSE 6.78 m; NMAD 2.37 m), followed by SRTM (5.03 m; 1.48 m) and EU-DEM (4.32 m; 1.44 m). The smallest discrepancies were found for TIN (RMSE 1.48 m; NMAD 0.41 m). These values relate to the models' agreement with the ALS, rather than to the independent, absolute accuracy of the ALS. The comparison also indicates that data integration in the EU-DEM reduced some of the discrepancies present in ASTER and SRTM.

Table 1. RMSE and NMAD [m] of the ASTER, SRTM, EU-DEM and TIN models relative to the reference ALS DTM.

Data	RMSE [m]	NMAD [m]
ASTER	6.78	2.37
SRTM	5.03	1.48
EU-DEM	4.32	1.44
TIN	1.48	0.41

The greatest differences with regard to ALS were observed in forested areas (Figure 6). The RMSE for ASTER reached 9.64 m there, whilst for the other satellite models it was around 6.6 m, and for TIN it was 2.67 m. In the other land-cover classes, the values were lower and more variable. The result confirms that surface characteristics influence model accuracy; however, due to the non-layered sampling scheme, differences between classes should be interpreted with caution.

The elevation range also varied between models. ASTER exhibited the widest range of values (132–248 m), whilst the ALS reference indicated a range of approximately 136–225 m (Table 2). Deviations in extreme values are significant as they may influence local gradients and, consequently, geomorphometric and hydrological derivatives.

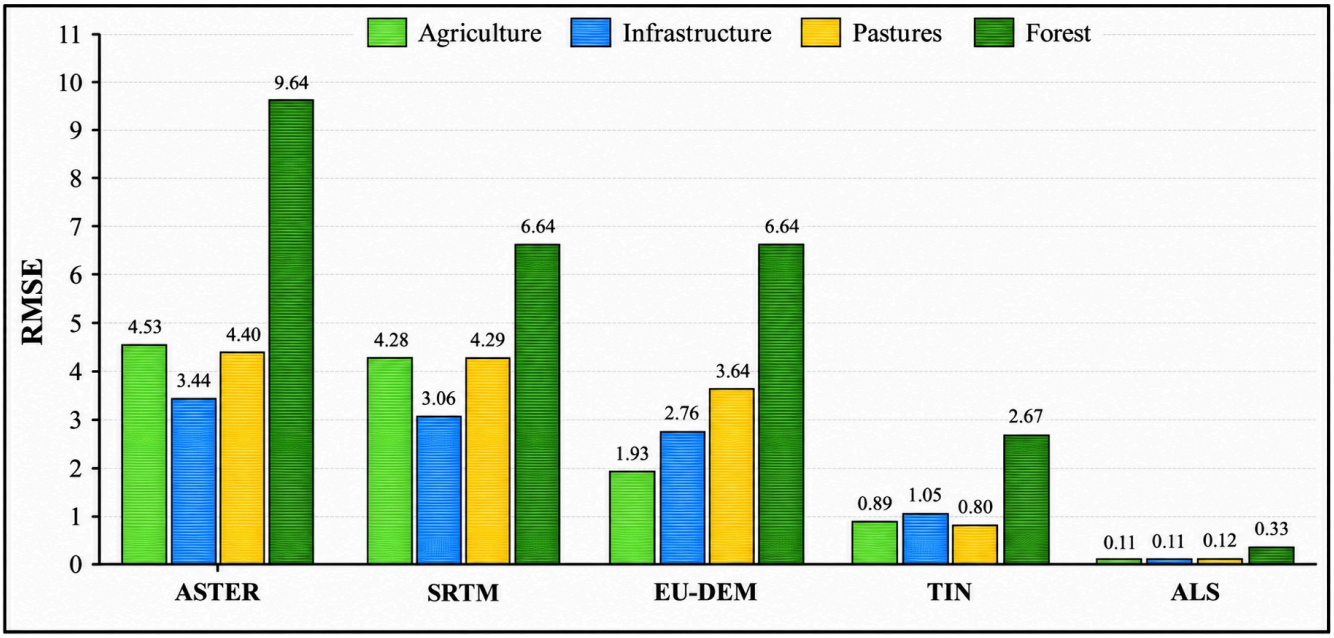

Figure 6. Variation in RMSE by land-cover class.

Table 2. Basic statistics for the digital elevation models under study.

Parameter	ASTER	SRTM	EU-DEM	TIN	ALS
Minimum height [m]	132	133	138.08	137.47	136.26
Maximum height [m]	248	223	223.11	223.23	225.02
Average height [m]	189.20	186.7	190.15	188.57	188.54
Average gradient [degrees]	6.16	3.30	2.46	5.34	6.63

3.2. Geomorphological Parameters

The hypsographic curves (Figure 7) followed a similar general trend, indicating that all models reproduce the main elevation pattern of the catchment. Local differences, however, are greater in the satellite-based models and are particularly evident in areas of highly dissected terrain. The ALS curve was used as a reference for assessing these deviations.

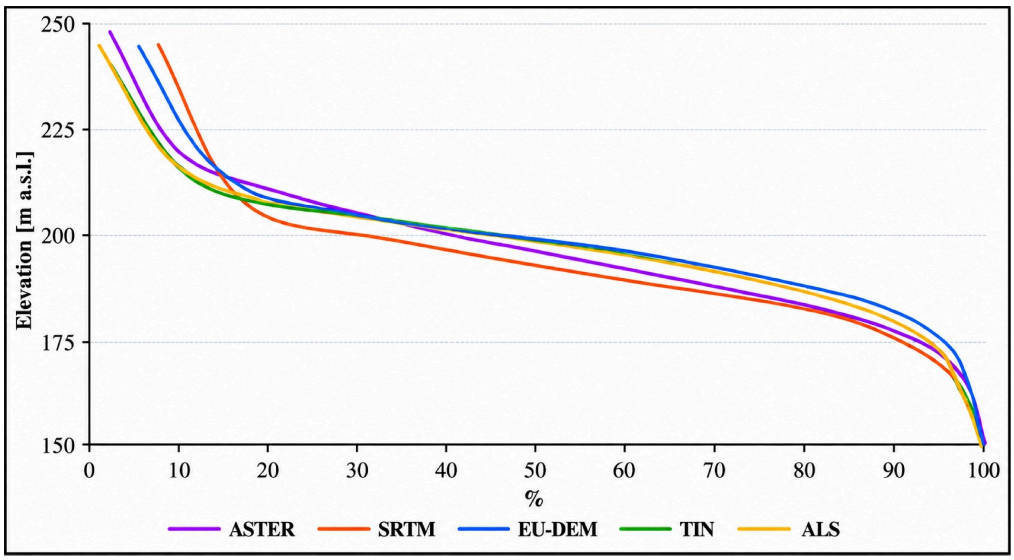

Figure 7. Hypsographic curves for ASTER, SRTM, EU-DEM, TIN and the reference ALS DTM.

Slope maps (Figure 8A–E) showed a stronger dependence on data quality and resolution than the hypsographic curves. Satellite models smoothed out the steep slopes of gorges and limited the range of high slope values. The TIN retained greater detail, but local model artefacts affected slope classification. This result is consistent with the dependence of DEM errors on slope and land cover observed in more recent validations [6,7,9]. In loess landscapes, detailed topographic information is particularly important for mapping the edges and axes of gullies; modern methods for mapping such features increasingly integrate remote-sensing imagery with DEMs and automatic classification algorithms [40].

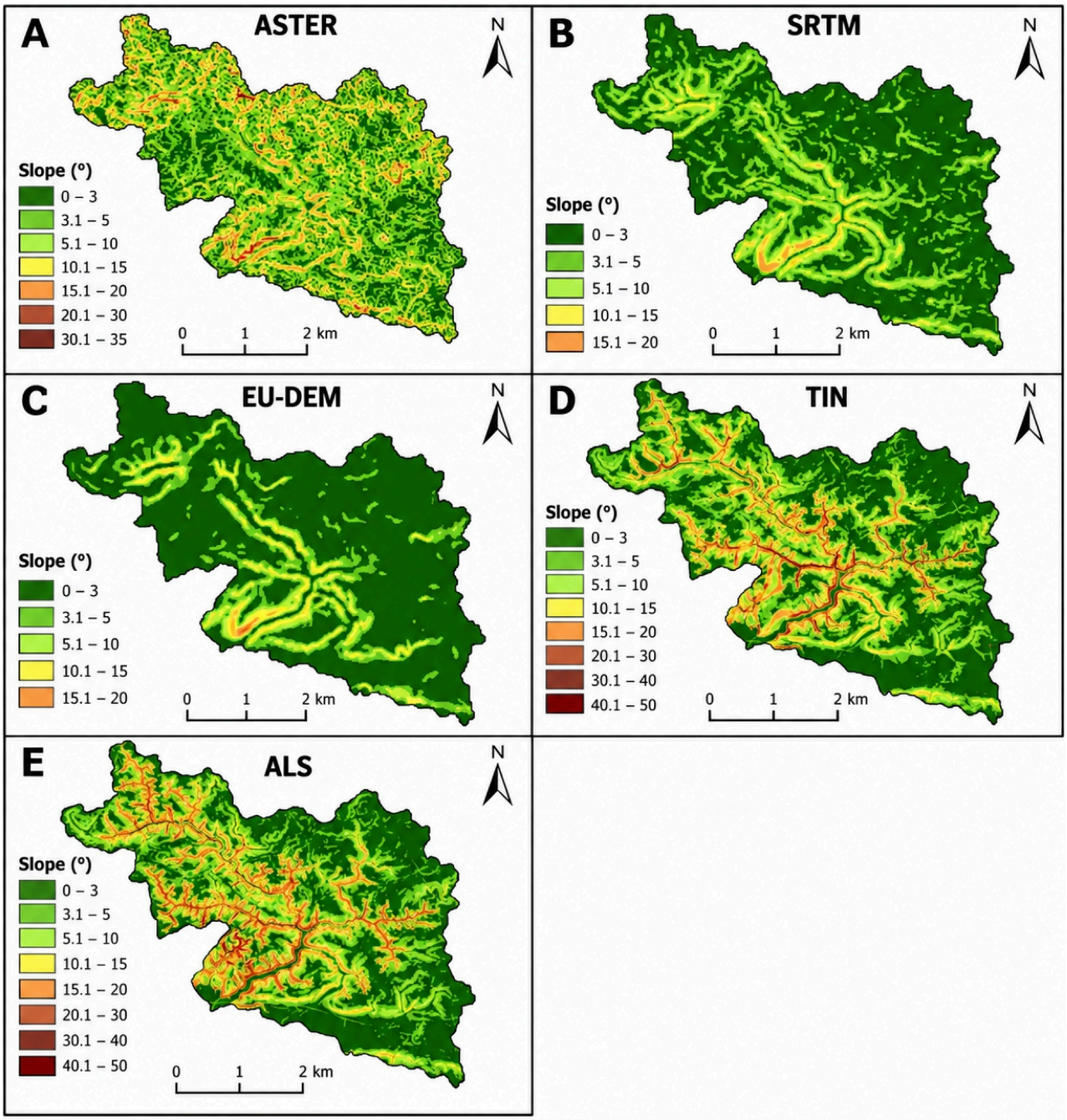

Figure 8. Slope maps derived from data: (**A**) ASTER, (**B**) SRTM, (**C**) EU-DEM, (**D**) TIN, (**E**) ALS as reference model.

Similar resolution-dependent generalization was visible in the aspect maps (Figure 9A–E), particularly within the gully network, although aspect differences relative to ALS were not quantified.

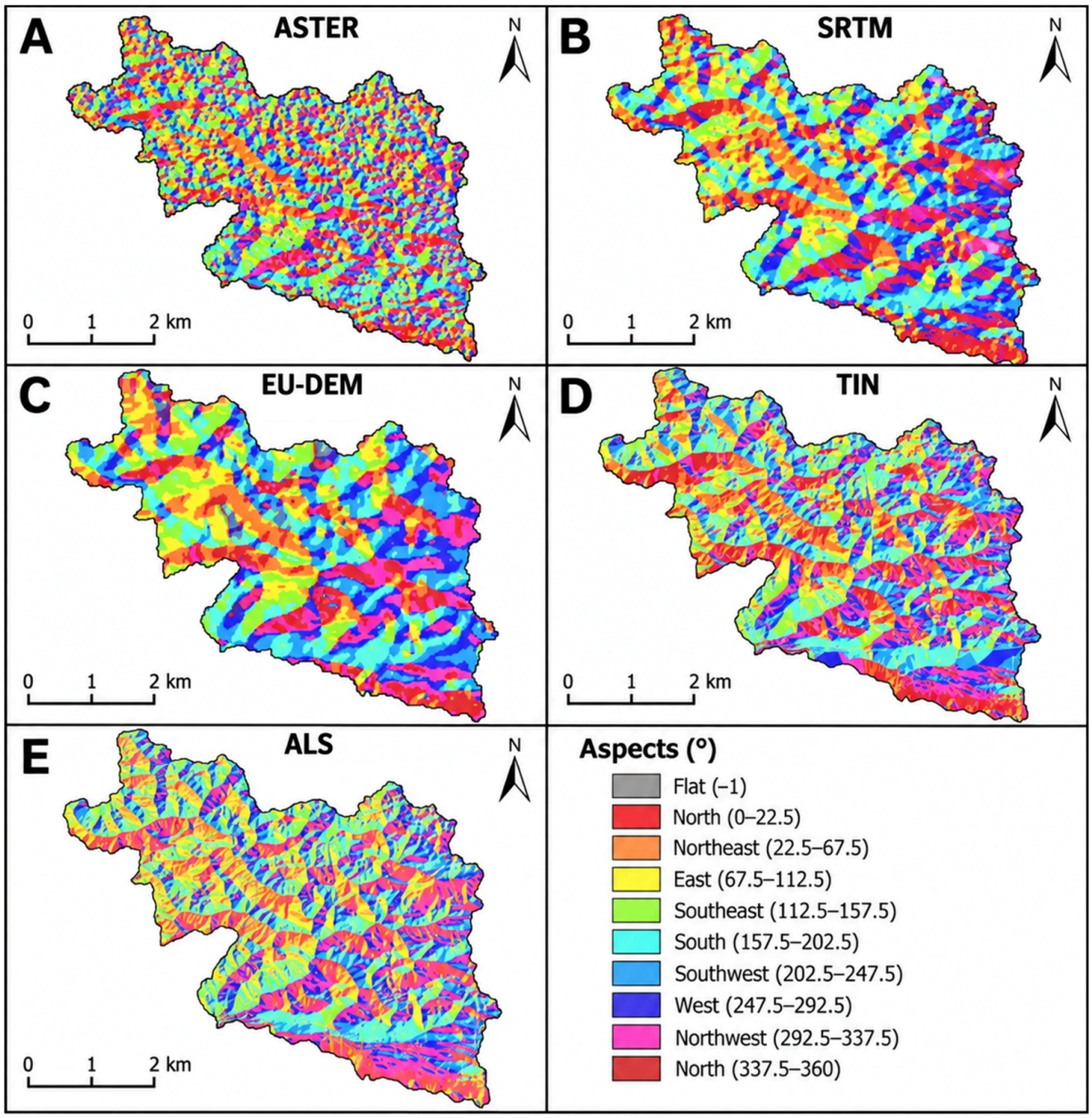

Figure 9. Aspect maps: (**A**) ASTER, (**B**) SRTM, (**C**) EU-DEM, (**D**) TIN, (**E**) ALS as a reference.

3.3. Hydrological Parameters

The drainage networks (Figure 10A–E) derived from the satellite models were highly generalized: their total length was approximately 11–13 km, whereas for the ALS 5-metre models it was approximately 65–68 km. A comparison with reference data (Figure 10E) shows that a resolution of approximately 25–30 m does not allow for the reliable representation of many short drainage lines and gully axes. This finding is consistent with more recent studies in which the quality of stream network delineation depended heavily on resolution, slope and land cover, rather than solely on the global vertical error measure [8]. In the case of loess catchments, this is of particular significance, as runoff and sediment transport can be highly concentrated within the gully system, and their dynamics vary

between rainfall and snowmelt events [20,41]. These differences should not be attributed solely to the DEM resolution or the method of terrain representation. Because a fixed threshold of 1000 accumulation cells was applied, the effective catchment area varied significantly depending on the DEM. Consequently, the length of the drainage network reflects both the generalization of the terrain and the cell-count-based extraction threshold. In loess catchments, this limitation is particularly significant, as surface runoff and sediment transport can be concentrated in gullies.

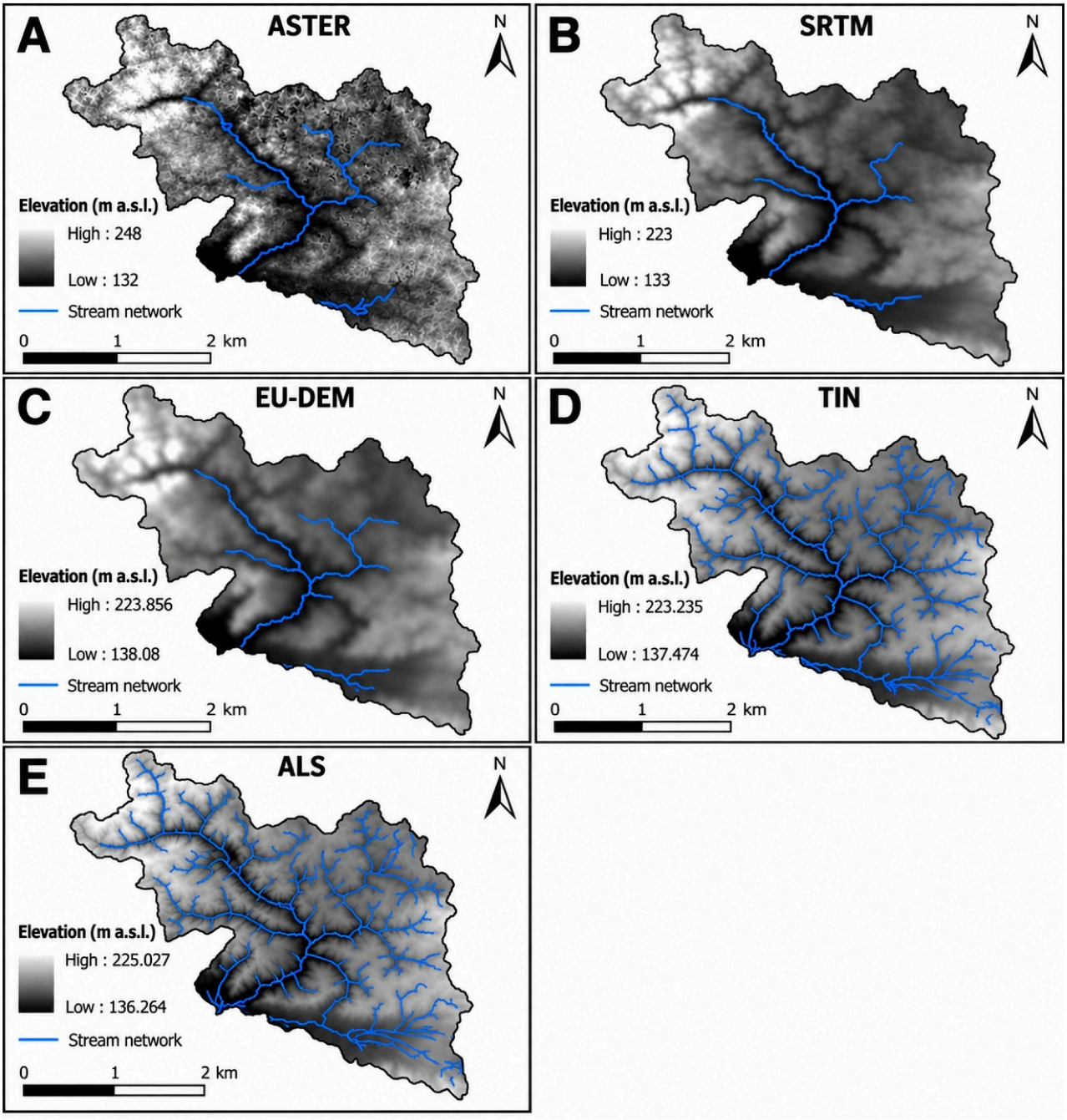

Figure 10. Drainage network delineated using an accumulation threshold of 1000 cells: (**A**) ASTER, (**B**) SRTM, (**C**) EU-DEM, (**D**) TIN, (**E**) ALS as reference.

The automatically delineated catchment boundaries (Figure 11A–E) differed among the elevation models and from the reference boundary. The delineated catchment areas were 11.94 km^2 for ASTER, 12.70 km^2 for SRTM, 11.98 km^2 for EU-DEM, 17.60 km^2 for

TIN, and 13.30 km^2 for ALS, compared with a reference catchment area of approximately 17.0 km^2. Most DEMs therefore underestimated the reference catchment area, whereas the TIN slightly overestimated it and locally included an additional section of terrain (Figure 11D). However, similarity in total catchment area should not be interpreted as full spatial agreement of the catchment boundaries, because local over- and underestimations may partly compensate for one another. These discrepancies indicate that even minor elevation errors in watershed areas can alter the output of the 'Watershed' algorithm.

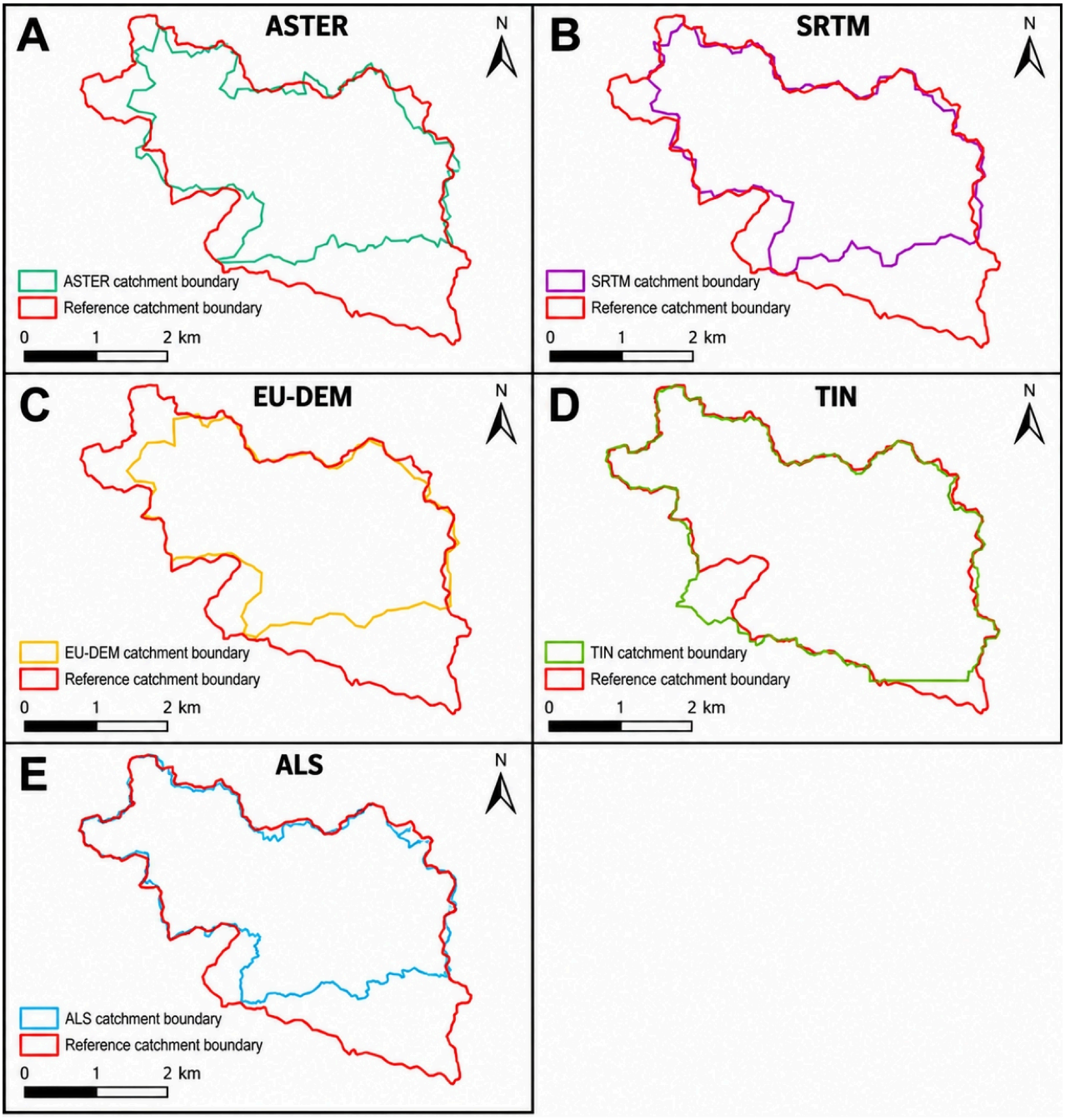

Figure 11. Automatically determined catchment boundaries superimposed on the reference boundary: (**A**) ASTER, (**B**) SRTM, (**C**) EU-DEM, (**D**) TIN, (**E**) ALS as reference.

3.4. Sediment Connectivity Index

SCI maps (Figure 12A–E) for all models indicated increased connectivity in valley floors and on gully slopes. However, the level of detail in the pattern clearly depended on

the elevation model. Models based on satellite data generalized both local topographic features and the drainage network, whereas the TIN model showed the greatest agreement with the ALS reference data (Figure 12E). As the SCI also depends on the C-coefficient and the chosen algorithm implementation, the results should not be interpreted as a direct measure of DEM 'accuracy'. Since the SCI is used in this study to validate the influence of topography, with all other input data held constant, we assessed how changing the elevation model modifies the spatial connectivity pattern relative to the ALS (Figure 12E).

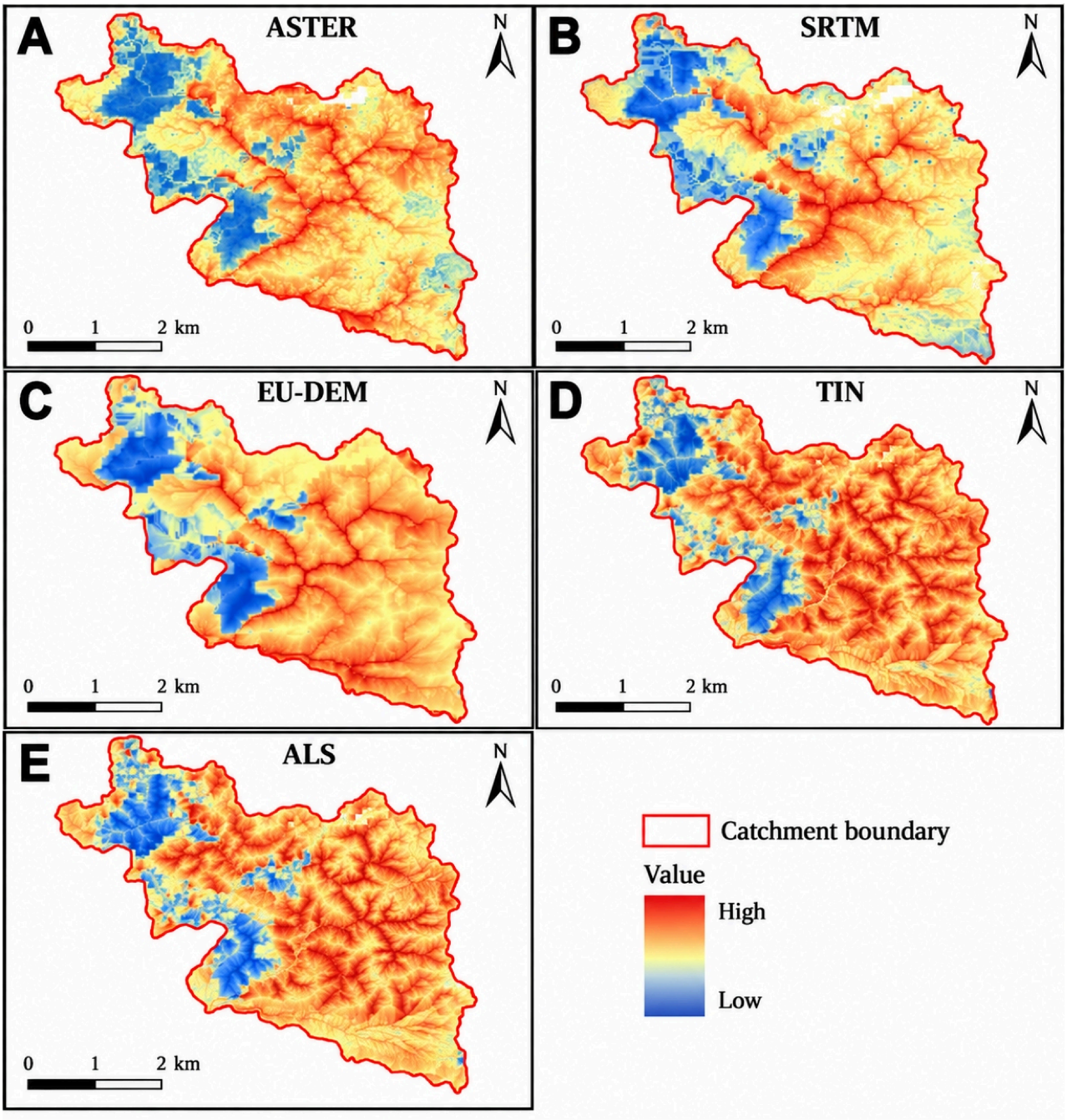

Figure 12. Sediment Connectivity Index (SCI): (**A**) ASTER, (**B**) SRTM, (**C**) EU-DEM, (**D**) TIN, (**E**) ALS as a reference.

4. Discussion

4.1. Altitudinal Consistency and the Role of ALS as Reference Data

In the study, a clear distinction was made between the models under assessment and the reference data. A DTM created from national ALS data from the ISOK project [18,32] was used as a common reference level for the evaluation of multi-source elevation models. The use of ISOK data as a reference for other LiDAR measurements also has a precedent in geomorphometric studies conducted for the study area [33]. The study was based on the assumption that DEM validation should rely on data more accurate than the product under assessment and on statistics robust to outliers [36]. This approach is consistent with extensive comparisons of global DEMs [3] and more recent validations utilizing ALS or high-quality reference data [6,7,9,11,12]. The larger elevation errors observed in forested areas may partly reflect the influence of vegetation canopies on global elevation products. Vegetation- and building-corrected products such as FABDEM [10] may reduce this effect. However, their performance in the Stocki Creek catchment would require independent validation against the ALS/LiDAR reference and was not evaluated in the present study.

4.2. Propagation of Elevation Data Uncertainty into Hydrological Modelling

Validation of derived products against ALS shows that the impact of DEM quality is not uniform across successive levels of analysis. The overall elevation distribution remains relatively stable, whilst products utilizing local gradients and the spatial continuity of the topography exhibit greater sensitivity to data quality and resolution. The hypsographic curves obtained for the individual models follow a similar pattern, whilst differences are more clearly evident in the slope, runoff organization and the structure of the drainage network. The results are consistent with previous studies indicating the influence of DEM quality and resolution on hydrological products [1,2,4,5,8].

Since the analyzed DEMs retained their original spatial resolution, this study did not experimentally separate the influence of spatial resolution from that of the data source and processing methods. The observed differences are therefore interpreted as the combined effect of the DEM source, processing characteristics, and original spatial resolution. The results obtained can be interpreted as the propagation of uncertainty through a hierarchical chain of products: elevation $\rightarrow$ slope $\rightarrow$ runoff routing $\rightarrow$ drainage network $\rightarrow$ sediment transport. The dependence of hydrological and geomorphometric products on the accuracy and resolution of the DEM is well documented, and the influence of the elevation model's characteristics can manifest itself both at the stage of determining topographic parameters and during runoff routing and sediment connectivity analysis [1,5,42,43]. The first level of this chain describes the consistency of the initial elevation field, while subsequent products utilize increasingly local information about elevation differences, gradients, and the topological continuity of runoff paths. As a result, even when the overall elevation pattern of a watershed remains similar, local errors or smoothing of the terrain can affect flow directions and how the drainage network is represented [1,2,8]. In the case of sediment connectivity analyses, the spatial resolution of the DEM is also important, as changes in pixel size can affect the values and spatial distribution of connectivity indices [42,43]. This does not imply a simple, linear increase in error at each stage, but rather indicates a growing sensitivity of processed products to the method of representing local topography.

This approach extends the classical DEM validation, which focuses primarily on assessing vertical accuracy using error statistics, including outlier-robust measures [3,6,36]. RMSE and NMAD are important for characterizing elevation consistency, but vertical accuracy alone does not directly determine whether an elevation product retains the spatial structure necessary for reliable reconstruction of drainage networks and hydrogeomorphological applications [2,8]. This is particularly evident when comparing drainage networks.

Satellite DEMs reflected the main watershed pattern. However, the drainage networks derived from them were significantly shorter. This contrast stems both from a less detailed representation of the terrain and from the use of a fixed accumulation threshold. This approach means that the observed differences in network length cannot be interpreted solely as a result of resolution. This finding is consistent with the broader observation that the suitability of a DEM for delineating stream networks cannot be assessed solely on the basis of its vertical accuracy, as the preservation of local topographic structure is also of significant importance [1,8]. This means that similarities in general elevation parameters do not necessarily translate into a comparable representation of the functional organization of runoff.

The importance of the spatial representation of input information is also increasingly emphasized in modelling that utilizes other types of remote-sensing data. Yu et al. [14], by integrating satellite rainfall data with a spatial model of runoff processes, demonstrated the importance of the appropriate localization and spatial representation of hydrological information for the quality of simulations. Although the mechanism of uncertainty is different in this case from that for DEMs, both approaches indicate that the practical value of an Earth Observation product depends not only on its nominal accuracy, but also on how the spatial information it represents influences subsequent stages of process modelling.

In the broader context of Earth Observation, a similar issue concerns the uncertainty generated and modified at successive stages of processing. Ma et al. [44] demonstrated, for multi-temporal Sentinel-2 classification, that the resulting product uncertainty depends on the configuration of the analytical process and the characteristics of the input data. Although their analysis concerns land-cover classification rather than elevation products, it illustrates a broader principle: the uncertainty of remote-sensing data should be considered in relation to the final product and the method by which it is derived, rather than solely in relation to the properties of the source data. In the case of hydrological modelling using a DEM, this implies the need to validate not only the elevations but also key derived products.

The SCI constitutes the final and most integrated element of the chain under analysis. It should be interpreted as an indicator of the spatial organization of potential pathways for water and sediment transfer, rather than as a direct measure of DEM accuracy. The index depends on both topography and the C-factor, as well as algorithm parameters [37,45]. Recent reviews emphasize the need to distinguish between structural and functional connectivity and to validate index results with process observations [46,47]. In the present study, however, maintaining a common C layer allows us to limit the variability of non-topographical input factors and to use the SCI to assess how a change in terrain representation modifies the spatial representation of a potential slope–gully–drainage network connection.

4.3. The Regional and Local Aspects of the Study in the Context of Short-Term Hydrological Events Reshaping the Network of Loess Gullies

In the Lublin Upland, the significance of short-term hydrological events for the development of gullies has been confirmed by long-term observations of runoff and sediment transport [20,41,48]. The results should therefore be interpreted not merely as a cartographic issue, but as a source of uncertainty in analyses of processes spatially concentrated within narrow erosional features. In loess landscapes, where a significant proportion of short runoff paths and slope–channel connections develop within gullies, the loss of local topographical information may have a disproportionately large impact on products describing the hydrological organization of catchment areas. Experimental studies in loess gullies showed that headcut retreat increases rapidly with time and flow discharge [49], while gully heads concentrate a substantial proportion of flow-energy expenditure, which is significantly related to sediment yield [50]. These findings indicate that small, spatially restricted topographic features may represent zones of disproportionate geomorphic activ-

ity. Consequently, their smoothing or omission in lower-resolution DEMs may affect the representation of hydrologically and geomorphologically meaningful flow pathways and slope–channel connections.

The main value of the study is therefore not to re-rank the accuracy of ASTER, SRTM, EU-DEM and TIN, but rather a cross-platform assessment demonstrating how the differences present in multi-source elevation products manifest themselves at successive levels of information—from elevation and local morphometry, through runoff organization and the drainage network, to the spatial pattern of sediment connectivity. The results indicate that elevation validation is a necessary but insufficient condition for assessing the suitability of DEMs in hydrological modelling. For such applications, it is equally important to validate derived products directly related to the process to be modelled. In this context, ALS data serve as an independent reference level, enabling the assessment not only of the elevation itself, but also of the implications of the choice of elevation product for further analyses.

5. Conclusions

The study involved a cross-platform assessment of multi-source elevation models, in which ASTER GDEM, SRTM, EU-DEM and TIN were validated against high-resolution ALS data, not only in terms of elevation but also with regard to products used in hydrological modelling and the assessment of sediment transport.

Of the models assessed, the smallest elevation discrepancies relative to ALS were found for the TIN (RMSE 1.48 m; NMAD 0.41 m), and the largest for ASTER (6.78 m; 2.37 m); EU-DEM and SRTM occupied an intermediate position. However, these results constitute a starting point for assessing uncertainty propagation, rather than the main interpretative finding of the study.

A comparison of the various models highlights the propagation of the influence of DEM quality and resolution through the chain: elevation → slope → runoff routing → drainage network → sediment connectivity. The overall elevation pattern of the catchment was relatively stable, whilst products more heavily dependent on local gradients and topographical continuity showed greater sensitivity to the choice of model.

Satellite models with a resolution of approximately 25–30 m are useful for identifying the general organization of the catchment, but in a highly fragmented loess landscape they smooth out steep features and generalize gullies and short runoff paths. Consequently, similar agreement at the level of the general elevation field does not guarantee an equally good representation of the hydrological structure.

The greatest elevation discrepancies were found in forested areas, which confirms that, when selecting data for hydrological modelling, spatial resolution, data acquisition technology and the nature of land cover must all be taken into account.

Among the evaluated models, the TIN showed the closest agreement with the ALS reference in reproducing the local topographic structure and drainage network, while the satellite-based DEMs exhibited greater deviations from the reference. However, the presence of local artefacts shows that the usefulness of an elevation product depends not only on its nominal resolution, but also on the quality of the input data and the model construction procedure.

A comparison of the SCI indicates that the choice of elevation model can alter the spatial representation of potential slope–gully–drainage network connections. The SCI is not a direct measure of DEM accuracy, but it demonstrates the consequences of topographical differences for an integrated product describing potential pathways for the transfer of water and sediment.

The results indicate that the assessment of the suitability of Earth Observation products in hydrology should not stop at the validation of raw data. The validation of derived models

directly related to the modelled process is necessary to determine whether the uncertainty of the input data remains acceptable after passing through subsequent modelling stages.

Author Contributions: Conceptualization, W.K. and I.Z.; methodology, W.K. and I.Z.; software, I.Z.; validation, W.K. and I.Z.; formal analysis, I.Z.; investigation, I.Z.; resources, I.Z.; data curation, I.Z.; writing—original draft preparation, W.K. and I.Z.; writing—review and editing, W.K. and I.Z.; visualization, W.K. and I.Z.; supervision, W.K.; project administration, W.K.; funding acquisition, W.K. All authors have read and agreed to the published version of the manuscript.

Funding: This research received no external funding.

Data Availability Statement: The original contributions presented in the study are included in the article. Further inquiries can be directed to the corresponding author.

Conflicts of Interest: The authors declare no conflicts of interest.

Abbreviations

ALS	Airborne Laser Scanning
ASTER	Advanced Spaceborne Thermal Emission and Reflection Radiometer
DEM	Digital Elevation Model
DTM	Digital Terrain Model
EO	Earth Observation
EPSG	European Petroleum Survey Group
ESDAC	European Soil Data Centre
ETRS89	European Terrestrial Reference System 1989
EU-DEM	European Digital Elevation Model
FABDEM	Forest And Buildings removed Copernicus Digital Elevation Model
GDEM	Global Digital Elevation Model
GRS80	Geodetic Reference System 1980
GUGiK	Head Office of Geodesy and Cartography
IC	Index of Connectivity
ISOK	IT System for the Protection of the Country against Extreme Hazards
JRC	Joint Research Centre
LiDAR	Light Detection and Ranging
LS	Slope Length and Steepness Factor
NMAD	Normalized Median Absolute Deviation
RMSE	Root Mean Square Error
RUSLE	Revised Universal Soil Loss Equation
SCI	Sediment Connectivity Index
SRTM	Shuttle Radar Topography Mission
TIN	Triangulated Irregular Network
WGS84	World Geodetic System 1984

References

1. Walker, J.P.; Willgoose, G.R. On the Effect of Digital Elevation Model Accuracy on Hydrology and Geomorphology. *Water Resour. Res.* **1999**, *35*, 2259–2268. [CrossRef]
2. Graf, L.; Moreno-de-las-Heras, M.; Ruiz, M.; Calsamiglia, A.; García-Comendador, J.; Fortesa, J.; López-Tarazón, J.A.; Estrany, J. Accuracy Assessment of Digital Terrain Model Dataset Sources for Hydrogeomorphological Modelling in Small Mediterranean Catchments. *Remote Sens.* **2018**, *10*, 2014. [CrossRef]
3. Uuemaa, E.; Ahi, S.; Montibeller, B.; Muru, M.; Kmoch, A. Vertical Accuracy of Freely Available Global Digital Elevation Models (ASTER, AW3D30, MERIT, TanDEM-X, SRTM, and NASADEM). *Remote Sens.* **2020**, *12*, 3482. [CrossRef]
4. Muthusamy, M.; Rivas Casado, M.; Butler, D.; Leinster, P. Understanding the Effects of Digital Elevation Model Resolution in Urban Fluvial Flood Modelling. *J. Hydrol.* **2021**, *596*, 126088. [CrossRef]
5. Li, J.; Chen, H.; Xu, C.-Y.; Li, L.; Zhao, H.; Huo, R.; Chen, J. Joint Effects of the DEM Resolution and the Computational Cell Size on the Routing Methods in Hydrological Modelling. *Water* **2022**, *14*, 797. [CrossRef]

6. Han, M.; Enwright, N.; Gesch, D.B.; Stoker, J.M.; Danielson, J.J.; Amante, C.J. Assessing the Vertical Accuracy of Digital Elevation Models by Quality Level and Land Cover. *Remote Sens. Lett.* **2024**, *15*, 667–677. [CrossRef]
7. Meadows, M.; Jones, S.; Reinke, K. Vertical Accuracy Assessment of Freely Available Global DEMs (FABDEM, Copernicus DEM, NASADEM, AW3D30 and SRTM) in Flood-Prone Environments. *Int. J. Digit. Earth* **2024**, *17*, 2308734. [CrossRef]
8. Marešová, J.; Bašta, P.; Gdulová, K.; Barták, V.; Kozhoridze, G.; Šmída, J.; Markonis, Y.; Rocchini, D.; Prošek, J.; Pracná, P.; et al. Choosing the Optimal Global Digital Elevation Model for Stream Network Delineation: Beyond Vertical Accuracy. *Earth Space Sci.* **2024**, *11*, e2024EA003743. [CrossRef]
9. Helmy, M.; Mandanici, E.; Vittuari, L.; Bitelli, G. Global Digital Terrain Models: Evaluation of Vertical Accuracy against Different Morphological Contexts. *Prog. Phys. Geogr. Earth Environ.* **2026**, *50*, 640–654. [CrossRef]
10. Hawker, L.; Uhe, P.; Paulo, L.; Sosa, J.; Savage, J.; Sampson, C.; Neal, J. A 30 m Global Map of Elevation with Forests and Buildings Removed. *Environ. Res. Lett.* **2022**, *17*, 024016. [CrossRef]
11. Liu, Z.; Zhu, J.; Fu, H.; Zhou, C.; Zuo, T. Evaluation of the Vertical Accuracy of Open Global DEMs over Steep Terrain Regions Using ICESat Data: A Case Study over Hunan Province, China. *Sensors* **2020**, *20*, 4865. [CrossRef] [PubMed]
12. Santillan, J.R. Vertical Accuracy Evaluation of the Forest and Buildings Removed Copernicus DEM (FABDEM) over the Philippines. *Int. Arch. Photogramm. Remote Sens. Spat. Inf. Sci.* **2023**, *48*, 311–318. [CrossRef]
13. Hong, D.; Hu, J.; Yao, J.; Chanussot, J.; Zhu, X.X. Multimodal Remote Sensing Benchmark Datasets for Land Cover Classification with a Shared and Specific Feature Learning Model. *ISPRS J. Photogramm. Remote Sens.* **2021**, *178*, 68–80. [CrossRef] [PubMed]
14. Yu, C.; Shao, H.; Hu, D.; Dai, X.; Wu, S. Runoff Simulation Modeling Method Integrating Spatial Element Dynamics and Neural Network for Remote Sensing Precipitation Data. *J. Hydrol.* **2024**, *642*, 131875. [CrossRef]
15. Rabus, B.; Eineder, M.; Roth, A.; Bamler, R. The Shuttle Radar Topography Mission—A New Class of Digital Elevation Models Acquired by Spaceborne Radar. *ISPRS J. Photogramm. Remote Sens.* **2003**, *57*, 241–262. [CrossRef]
16. Abrams, M.; Crippen, R.; Fujisada, H. ASTER Global Digital Elevation Model (GDEM) and ASTER Global Water Body Dataset (ASTWBD). *Remote Sens.* **2020**, *12*, 1156. [CrossRef]
17. Schumann, G.J.-P.; Bates, P.D. The Need for a High-Accuracy, Open-Access Global DEM. *Front. Earth Sci.* **2018**, *6*, 225. [CrossRef]
18. Woźniak, P. High Resolution Elevation Data in Poland. In *Geomorphometry for Geosciences*; Adam Mickiewicz University: Poznań, Poland, 2015; pp. 13–14.
19. Gawrysiak, L.; Harasimiuk, M. Spatial Diversity of Gully Density of the Lublin Upland and Roztocze Hills (SE Poland). *Ann. UMCS Sect. B* **2012**, *67*, 27–43. [CrossRef]
20. Rodzik, J.; Furtak, T.; Zgłobicki, W. The Impact of Snowmelt and Heavy Rainfall Runoff on Erosion Rates in a Gully System, Lublin Upland, Poland. *Earth Surf. Process. Landf.* **2009**, *34*, 1938–1950. [CrossRef]
21. Dotterweich, M.; Rodzik, J.; Zgłobicki, W.; Schmitt, A.; Schmidtchen, G.; Bork, H.-R. High Resolution Gully Erosion and Sedimentation Processes, and Land Use Changes since the Bronze Age and Future Trajectories in the Kazimierz Dolny Area (Nałęczów Plateau, SE-Poland). *CATENA* **2012**, *95*, 50–62. [CrossRef]
22. Superson, J.; Rodzik, J.; Reder, J. Natural and Human Influence on Loess Gully Catchment Evolution: A Case Study from Lublin Upland, E Poland. *Geomorphology* **2014**, *212*, 28–40. [CrossRef]
23. Zgłobicki, W.; Rodzik, J.; Superson, J.; Dotterweich, M.; Schmitt, A. Phases of Gully Erosion in the Lublin Upland and Roztocze Region. *Ann. UMCS Sect. B* **2014**, *69*, 149–162. [CrossRef]
24. Superson, J.; Rodzik, J.; Reder, J.; Zgłobicki, W.; Klimowicz, Z.; Franczak, Ł. Phases of Alluvial Fan Development in a Loess Area, Lublin Upland, E Poland. *Quat. Int.* **2016**, *399*, 31–45. [CrossRef]
25. Kondracki, J. *Geografia Regionalna Polski*, 3rd ed.; Wydawnictwo Naukowe PWN: Warszawa, Poland, 2002.
26. Rodzik, J.; Krukowski, M.; Zagórski, P. The Mechanism and Stages of Development of a Field Road Gully in Relation to Changes in the Surrounding Land Relief. *Ann. UMCS Sect. B* **2014**, *69*, 135–147. [CrossRef]
27. Rejman, J.; Rafalska-Przysucha, A.; Rodzik, J. The Effect of Land Use Change on Transformation of Relief and Modification of Soils in Undulating Loess Area of East Poland. *Sci. World J.* **2014**, *2014*, 341804. [CrossRef] [PubMed]
28. Zgłobicki, W. Present and Past Sedimentation Rates in Loess Areas of the Lublin Upland (E Poland). *Géomorphol. Relief Process. Environ.* **2013**, *19*, 79–92. [CrossRef]
29. Rodzik, J.; Gajek, G.; Zgłobicki, W. Loess Gullies of the Nałęczów Plateau—An Outcome of Human–Environment Interactions. In *Landscapes and Landforms of Poland*; Springer International Publishing: Cham, Switzerland, 2024; pp. 457–468. [CrossRef]
30. Rodzik, J.; Żuraw, B.; Sowińska-Świerkosz, B.; Kuna, J.; Sosnowska, M.; Podsiedlik, M. Multi-Criteria Evaluation for the Sustainable Use of Loess Gullies in Rural–Urban Borderline. *Sci. Rep.* **2025**, *15*, 10801. [CrossRef] [PubMed]
31. EU-DEM v1.1—Dataset Documentation and Archive. Available online: https://cis2.eea.europa.eu/data/42/ (accessed on 9 September 2026).

32. *Podsumowanie Działań Głównego Urzędu Geodezji i Kartografii w Zakresie Produkcji i Wykorzystania Danych Przestrzennych w Latach 2010–2015*; Główny Urząd Geodezji i Kartografii (GUGiK): Warszawa, Poland, 2015. Available online: https://www.gugik.gov.pl/__data/assets/pdf_file/0006/34098/Podsumowanie-dzialan-GUGiK-w-zakresie-danych-ALS.pdf (accessed on 11 September 2026).
33. Bartmiński, P.; Siłuch, M.; Kociuba, W. The Effectiveness of a UAV-Based LiDAR Survey to Develop Digital Terrain Models and Topographic Texture Analyses. *Sensors* **2023**, *23*, 6415. [CrossRef] [PubMed]
34. Kociuba, W.; Janicki, G.; Rodzik, J.; Stępniewski, K. Comparison of Volumetric and Remote Sensing Methods (TLS) for Assessing the Development of a Permanent Forested Loess Gully. *Nat. Hazards* **2015**, *79*, 139–158. [CrossRef]
35. Khan, S.; Bartley, R.; Kinsey-Henderson, A.E.; Hawdon, A. Assessing Gully Erosion and Rehabilitation Using Multi Temporal LiDAR DEMs: Case Study from the Great Barrier Reef Catchments, Australia. *Int. Soil Water Conserv. Res.* **2024**, *12*, 184–199. [CrossRef]
36. Höhle, J.; Höhle, M. Accuracy Assessment of Digital Elevation Models by Means of Robust Statistical Methods. *ISPRS J. Photogramm. Remote Sens.* **2009**, *64*, 398–406. [CrossRef]
37. Borselli, L.; Cassi, P.; Torri, D. Prolegomena to Sediment and Flow Connectivity in the Landscape: A GIS and Field Numerical Assessment. *CATENA* **2008**, *75*, 268–277. [CrossRef]
38. Cavalli, M.; Trevisani, S.; Comiti, F.; Marchi, L. Geomorphometric Assessment of Spatial Sediment Connectivity in Small Alpine Catchments. *Geomorphology* **2013**, *188*, 31–41. [CrossRef]
39. Panagos, P.; Borrelli, P.; Meusburger, K.; Alewell, C.; Lugato, E.; Montanarella, L. Estimating the Soil Erosion Cover-Management Factor at the European Scale. *Land Use Policy* **2015**, *48*, 38–50. [CrossRef]
40. Wang, Z.; Zeng, R.; Ma, P. Determining of Gully Erosion Susceptibility Based on UAV and Machine Learning in Loess Plateau. *Geomat. Nat. Hazards Risk* **2024**, *15*, 2421382. [CrossRef]
41. Janicki, G.; Rodzik, J.; Stępniewski, K.; Kociuba, W. Influence of the Precipitation Pattern on the Water Runoff Dynamics from the Loess Gully in the Lublin Upland (Eastern Poland) in the Years 2003–2022. *Quaest. Geogr.* **2025**, *44*, 39–56. [CrossRef]
42. Cantreul, V.; Bielders, C.; Calsamiglia, A.; Degré, A. How Pixel Size Affects a Sediment Connectivity Index in Central Belgium. *Earth Surf. Process. Landf.* **2018**, *43*, 884–893. [CrossRef]
43. Zou, W.; Xin, Z. The Optimal DEM Resolution for Determining Sediment Connectivity at Runoff Plot Scale. *Soil Tillage Res.* **2025**, *254*, 106700. [CrossRef]
44. Ma, L.; Schmitt, M.; Zhu, X. Uncertainty Analysis of Object-Based Land-Cover Classification Using Sentinel-2 Time-Series Data. *Remote Sens.* **2020**, *12*, 3798. [CrossRef]
45. Turley, M.; Hassan, M.A.; Slaymaker, O. Quantifying Sediment Connectivity: Moving toward a Holistic Assessment through a Mixed Methods Approach. *Earth Surf. Process. Landf.* **2021**, *46*, 2501–2519. [CrossRef]
46. Hooke, J.M.; Souza, J.O.P. Challenges of Mapping, Modelling and Quantifying Sediment Connectivity. *Earth-Sci. Rev.* **2021**, *223*, 103847. [CrossRef]
47. Martini, L.; Cavalli, M.; Picco, L. Predicting Sediment Connectivity in a Mountain Basin: A Quantitative Analysis of the Index of Connectivity. *Earth Surf. Process. Landf.* **2022**, *47*, 1500–1513. [CrossRef]
48. Rodzik, J.; Janicki, G.; Stępniewski, K.; Kociuba, W. Variability of Suspended Sediment Runoff as an Expression of the Long-Term Dynamics of Loess Gully Development—An Example from the Lublin Upland (Eastern Poland). *Land* **2024**, *13*, 2222. [CrossRef]
49. Shi, Q.; Wang, W.; Guo, M. Headcut erosion characteristics revealed through simulated rainfall and scouring experiments in the gully region of the Loess Plateau. *J. Soil Water Conserv.* **2022**, *77*, 172–183. [CrossRef]
50. Shi, Q.; Wang, W.; Feng, L. Response of the headcut erosion process to flow energy variation in the Loess gully region of China. *Water* **2022**, *14*, 3038. [CrossRef]

Disclaimer/Publisher's Note: The statements, opinions and data contained in all publications are solely those of the individual author(s) and contributor(s) and not of MDPI and/or the editor(s). MDPI and/or the editor(s) disclaim responsibility for any injury to people or property resulting from any ideas, methods, instructions or products referred to in the content.